Processing of Functional Texturing on Micro-fibers by Laser-induced Micro/Nanoscale Surface Topographies

Masaki Ysmaguchi, Ryosuke Kase, and Hidenori Shimada

Graduate School of Medicine, Science & Technology, Shinshu University, 3-15-1, Tokida, Ueda 386-8567, Japan
E-mail: masakiy@shinshu-u.ac.jp

The purpose of this study was to establish a method for fabricating a laser-induced micro/nanoscale surface topography (micro/nanotopography) on micro-fibers of glass (quartz) with a diameter of 125 μm by using a femtosecond-pulsed laser to express the function of hydrophilicity. The micro/nanotopographies were produced through laser ablation by using a femtosecond-pulsed laser with a wavelength of 514 nm, a pulse width of 234 fs, a repetition rate of 60 kHz, and a spot diameter of 6.9 μm. Structures of the irradiated surfaces were observed experimentally using a scanning electron microscope. A micro/nanotopography was observed on the surface of the micro-fiber when fluence and/or overlap ratio exceeded a given threshold. These experimental data showed evidence of a micro/nanotopography on laser-ablated micro-fibers. The apparent contact angles ranged from 106.4° to 88.7° without the micro/nanotopography, and decreased from 88.2° to 48.7° when a micro/nanotopography was presented. In particular, several cases of hydrophilicity under 51.1° were obtained, likely because of the non-continuous change in wettability from the Cassie state to the Wenzel state. Thus, optimum conditions for including both a micro/nanotopography and a hydrophilic surface on a micro-fiber were identified.

DOI: 10.2961/jlmn.2020.02.2008
Keywords: femtosecond-pulsed laser, micro/nanoscale surface topography, fiber, hydrophilicity, hierarchical structure, Cassie-Baxter equation

1. Introduction

The comfort of clothing is determined by the material used and design-related factors [1]. Wetness on the surface of the skin-clothing interface affects the wearer's comfort. Thus, textures on the surface of fibers are useful for a variety of features of textiles, including hydrophobicity, hydrophilicity, moisture retention, breathability, dyeability, cushioning, and touch. These surface topographies can be called functional textures. Bahners *et al*. proposed a characteristic modification of the surface topography of highly absorbent and oriented synthetic fibers after irradiation using several excimer laser pulses [2-3]. However, it is difficult to process micro- and nano-textures on fibers with micron-scale diameters based on their thermomechanical behavior due to the risk of rupture [4].

A number of methods have been proposed for surface modification due to laser irradiation. In 1965, Birnbaum discovered that a periodic structure with damage at the wavelength scale was created at the bottom of the processing marks of lasers [5]. Since then, many laser-induced surface structures, both random [6-7] and periodic [8-10], have been reported. Pulsed laser sources such as nanosecond- [11], picosecond- [12], and femtosecond-pulsed lasers [13] can be used to create various structures. It is important when fabricating micro/nanoscale surface topographies to control such conditions of the laser as pulse width and fluence.

Femtosecond-pulsed lasers can be used to create a variety of micro- and nano-structures in the open environment without lubricating oil, dust, heat exhaust, and noise than conventional machine tools [14]. The main feature of the femtosecond-pulsed laser is a clear ablation threshold. Compared with the nanosecond-pulsed laser, the femtosecond-pulsed laser has the additional capability of minimizing thermal damage [15].

Biomimetic surfaces have been developed to improve such properties of wettability as liquid repellency, adhesion, self-cleaning, and drag reduction [16-18]. Hydrophilic surfaces can be produced by mimicking hierarchical structures at the micro- and nano-scales of carnivorous plants such as *Nepenthes* [19-20]. The contact angle, θ, is a parameter, that characterizes the hydrophobicity/hydrophilicity of a solid surface.

The purpose of this study was to establish a method for inducing a micro/nanoscale surface topography (micro/nanotopography) on micro-fibers by a femtosecond-pulsed laser to represent the function of hydrophilicity. The authors carried out fabrication of hierarchical structures on a micro-fiber using a femtosecond-pulsed laser to this end. The wetting behavior in equilibrium and the apparent contact angles were assessed using equipment fabricated for the micro-fiber. The optimum conditions of direct processing exhibiting hydrophilicity were demonstrated experimentally. Additionally, theoretical considerations were performed qualitatively.

2. Materials and Methods

2.1 Laser processing

A glass micro-fiber (quartz, 125 μm cladding diameter, Furukawa Electric Co., Ltd., Japan) was used as the test-piece to generate hierarchical structures on the surface. The equilibrium contact angle of the material was 18° according to a dip method that defined a surface with zero curvature [21].

A commercial femtosecond-pulsed laser (Carbide, Light conversion UAB, Republic of Lithuania) that provided pulses at an oscillatory wavelength of 514 nm, at a pulse width of 234 fs, and a repetition rate of 60 kHz, was used for the experiment (Fig.1). A laser beam with a Gaussian profile was focused perpendicularly on to the micro-fibers using a beam expander (×3, S6EXZ5311/292, Sill Optics GmbH & Co. KG, Germany), using a condenser lens (focal length: f = 40.2 mm, Sigmakoki Co. Ltd., Saitama, Japan), and an automatic *xyz*-stage (± 0.5 μm positioning accuracy, HST-50XY and OSMS60-10ZF, Sigmakoki Co. Ltd.). The scanning velocity was 0.5 mm/s in both directions. The spot diameter at the focal point on the micro-fiber surface was calculated at 6.9 μm by full width at half maximum (FWHM) using a laser beam quality factor M^2 = 1.2 and an expanded laser beam diameter of 4.56 mm [22].

Twenty-five micro-fiber samples were fabricated using the parameters of fluence, F, ranging from 2.34 J/cm^2 to 18.36 J/cm^2, and an overlap ratio of laser spots, OR, ranging from 0% to 90% (Table 1). The pitch of each spot, τ ($\tau_x = \tau_y$), ranged from 0.7 – 7 μm, with a maximum value set to be equal to the diameter of the laser beam.

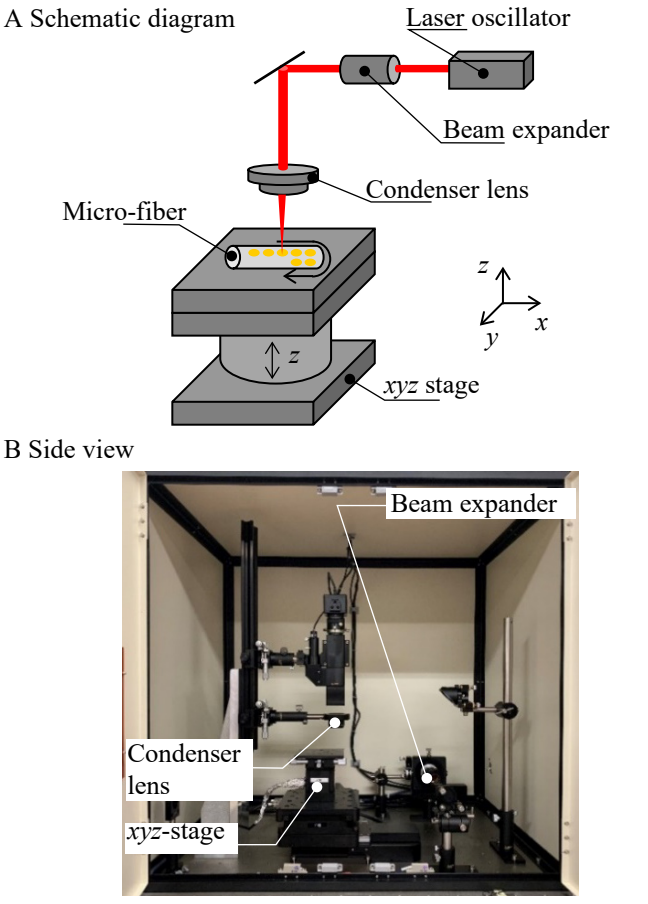

Fig. 1 Laser processing system of LIPPS on a micro-fiber surface using a femtosecond-pulsed laser.

Table 1 Overlap ratio of laser spots used for the fabrication.

Overlap ratio (%)	0	30	50	70	90
Pitch τ (μm)	7	4.9	3.5	2.1	0.7
Directions x, y					

2.2 Measurement of surface structure

Various surface geometries of the micro-fibers were compared with the experimental observations using a scanning electron microscope (SEM; JEM-6010LA, JEOL Ltd., Japan). The surface area was measured perpendicularly using a non-contact laser confocal microscope (10 nm resolution for depth, OLS4100, Olympus Co., Japan). The surface area ratio, SA, was calculated from the ratio of the surface area before to that after laser processing for each micro-fiber as follows:

$$\text{SA ratio} = \frac{Surface\ area\ after\ laser\ manufactureing}{Surface\ area\ before\ laser\ manufactureing} \quad (1)$$

The surface areas of the micro-fibers were measured from the vertical direction (Fig.2). The range of measurements in the circumferential and the longitudinal directions were 90° and 100 μm, respectively.

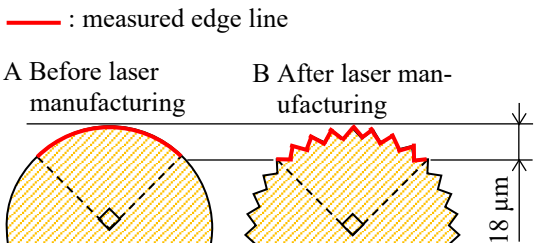

Fig. 2 Measurement areas of surface area ratio.

2.3 Apparent contact angle

The apparent contact angles of the micro-fibers were measured using a commercial contact angle analyzer (DM-701, Kyowa Interface Science Co. Ltd., Japan) by dropping 1 μL of a distilled water droplet from a microsyringe between two micro-fibers using a fabricated fixing jig of micro-fibers (Fig.3). The measurements were repeated for five times (n = 5), and the mean values were used. The distance between the micro-fibers was set to 500 μm to prevent the generation of a capillary force.

3. Results and Discussion

3.1 Measurement of surface structure

Table 2 shows the results for the surface structures of the micro-fibers as observed by the SEM. Periodic and circular dimples were observed when the OR ratio was 0%. A random topography at the micro- and sub-nano-scales appeared on the surface of the micro-fibers when the energy of the laser exceeded a threshold level determined by the fluence and/or the OR ratio (the results were within the red solid line). The micro-fiber ruptured when F > 18.36 J/cm^2 and OR > 70%.

The SA ratio without the micro/nanotopography was in the range 0.98 – 1.28. The SA ratio with the micro/nanotopography condition was in the range 1.28 – 3.12. It reached its maximum at 4.46 J/cm^2 of fluence and 90% of the OR ratio. This increase in the SA ratio supported the inducement due to the micro/nanotopography.

A Measurement method

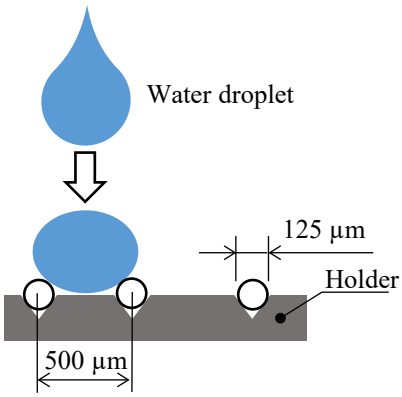

B Side view

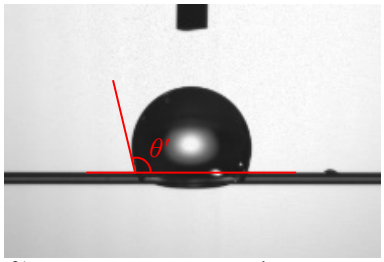

θ': apparent contact angle

C Top view

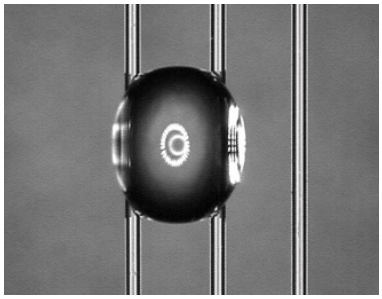

Fig. 3 Schematic diagram of equipment used for the measurement of the apparent contact angle.

3.2 Apparent contact angle

Before laser processing, the apparent contact angle of the micro-fiber was 113.2° (n = 5), which agreed well with the calculation results of the Cassie–Baxter equation with a cylindrical model [23].

After laser processing, the apparent contact angles without the micro/nanotopography ranged from 106.4° to 88.7°, and decreased from 88.2° to 48.7° in case of a micro/nanotopography (the results were within the red solid line, Table 3). It was possible that a part of these topographies formed a hierarchical structure. In particular, hydrophilicities under 51.1° were achieved under the three conditions within the solid line in Table 3. These results showed that water reached the bottom of the texture because it was introduced using the fabricated hierarchical structures. It was estimated that surface wettability transitioned from the Cassie state to the Wenzel stable state owing to a non-continuous change in wettability because hydrophilicity had developed.

When the grooves were filled with water (Wenzel state, Fig.4), the relationship between the apparent contact angles, θ', and the geometry of the surface structure can be expressed based on the Cassie-Baxter equation as follows [24-25]:

$$\cos\theta' = 1 + f\,(\cos\theta - 1) \qquad (2)$$

where f is the ratio of the fractional area, $f = \frac{f_1}{f_1 + f_2}$.

Fig.5 shows the calculated results of the ratio of the fractional area, f, obtained using measured results of the apparent contact angles, θ', for 10 cases of micro-fibers with the micro/nanotopography (the results were within the blue solid line in Table 3). The apparent contact angles decreased correspondingly when the value of f decreased. The value of f ranged between 0.24 – 0.27 when the hydrophilicities were under 51.1°. These tendencies were derived from Eq. (2).

Table 2 Measured results of micro-fibers for surface structures according to SEM.

Fluence F (J/cm^2)	Overlap ratio, OR (%) 0	30	50	70	90
2.34	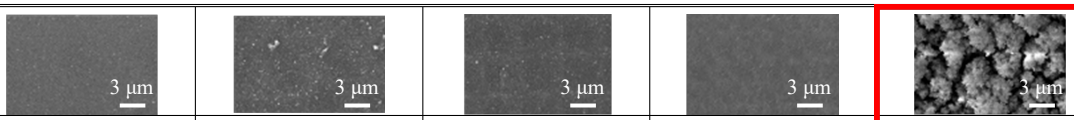				
4.46	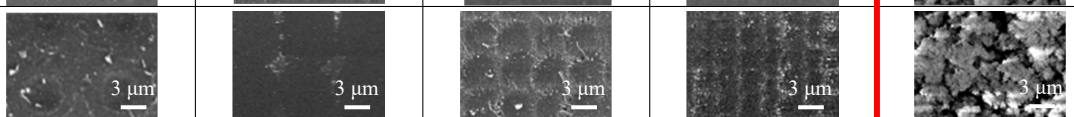				
8.88	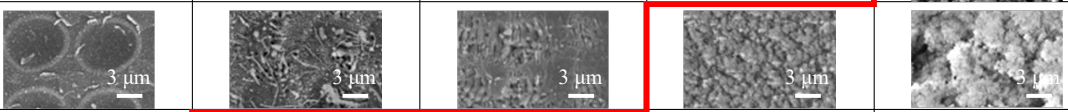				
13.69	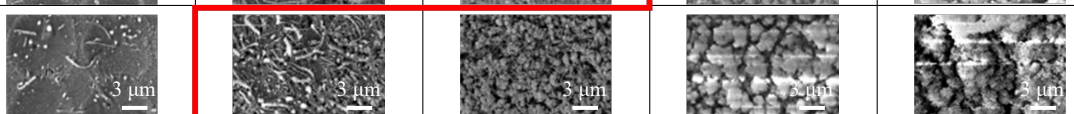				
18.36	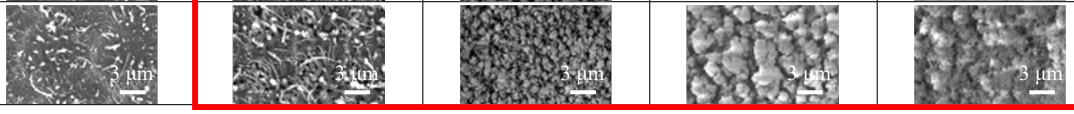				

(OR: overlap ratio; F: fluence; ▬: surfaces with micro/nanotopography)

Table 3 Measured results of the apparent contact angles of the micro-fibers.

Fluence F (J/cm^2)	Overlap ratio, OR (%) 0	30	50	70	90
2.34	106.4°	105.6°	96.6°	102.0°	80.7°
4.46	95.8°	94.7°	94.1°	89.0°	51.1°
8.88	90.8°	90.6°	90.3°	87.6°	49.5° (81.2°)
13.69	88.7°	88.2°	85.7°	86.3°	48.7°
18.36	89.1°	81.4°	85.5°	— (Broken)	— (Broken)

(Equilibrium contact angle on micro-fiber θ = 113.2°, ——: hydrophilic surfaces, ——: data used for the calculation in Fig.5 using Eq. (2))

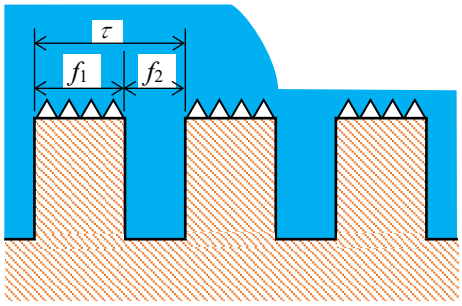

Fig. 4 Schematic of a surface with hierarchical structure.

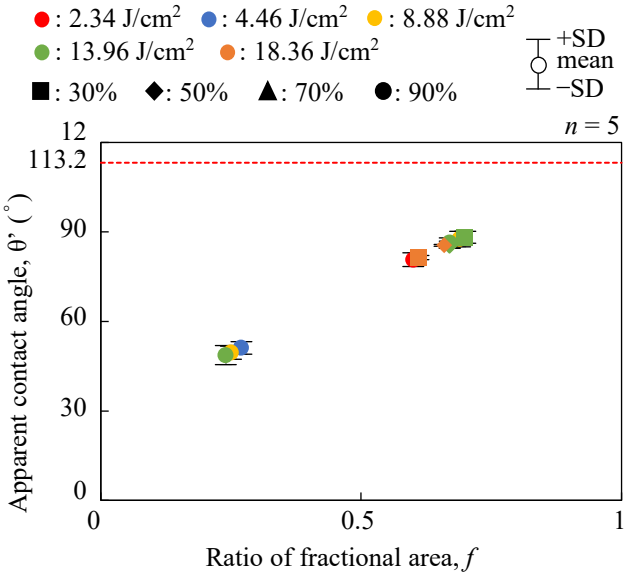

Fig. 5 Calculated results of the ratio of fractional area, f, using the measured results of apparent contact angles, θ', for 10 cases of micro-fibers with micro/nanotopography (the results were within the blue solid line in Table 3, SD: standard deviation).

However, Eq. (2) does not consider the roughness of surface f_1. It was clear from the SEM images that the processing area provided with the reduction of the apparent contact angle had more significant surface structures. Hierarchical structures appeared in the three conditions when the hydrophilicities were under 51.1° (the results were within the red solid line, Table 3), causing the hydrophilicity to become prominent in the textures.

4. Conclusion

The experimental data showed evidence of a micro/nanotopography on the laser-ablated micro-fibers. They were used to identify the optimum conditions for inducing a micro/nanotopography and a hydrophilic surface on a micro-fiber. Although it was difficult to measure the three-dimensional structure in the nanometer range, we estimated the structures from SEM images and hydrophilicities. With regard to the hydrophilicity of micro-fibers, the hierarchical structures exhibited a reduction in the apparent contact angles from 113.2° to 48.7°.

Fabrics with high absorbency, such as cotton, are smooth to touch. There is benefit in modifying the properties of chemical fibers to render them similar to those of natural fibers. In this research, we used the vertical direction, which might be applicable to the treatment of the flat surface of fabrics.

Improvements may be needed for using the proposed method for oils and other complex liquids because they are dominant in living environments.

Acknowledgments

This work was supported in part by grant no. 20H04514 from the Japan Society for the Promotion of Science, and was based on the ultra-sensitive and rapid cancer testing technique based on fiber-type amplification (P.I. M. Yamaguchi).

References

[1] M. Raccuglia, B. Sales, C. Heyde, G. Havenith, and S. Hodder: Appl. Ergon., 73, (2018) 33.
[2] T. Bahners and E. Schollmeyer: Angew. Makromol. Chem., 151, (1987) 19. (in Germany)
[3] T. Bahners, W. Kesting, and E. Schollmeyer: Appl. Surf. Sci., 69, (1993) 12.
[4] T. Bahners: Opt. Quant. Electron., 27, (1995) 1337.
[5] R. Birnbaum: J. Appl. Phys., 36, (1965) 3688.
[6] C.D. Marco, S.M. Eaton, M. Levi, G. Cerullo, S. Turri, and R. Osellame: Langmuir, 27, (2011) 8391.
[7] D.H. Kam, S. Bhattacharya, and J. Mazumder: J. Micromech. Microeng., 22, (2012) 105019.
[8] J.F. Young, J.E. Sipe, and H.M. van Driel: Opt. Lett., 8, (1983) 431.
[9] A.M. Bonch-Bruevich, M.N. Libenson, V.S. Markin, and V. Trubaev: Opt. Eng., 31, (1992) 718.
[10] D.C. Emmony, R.P. Howson, and L.J. Willis: Appl. Phys. Lett., 23, (1973) 598.
[11] S. Gupta and P. Molian: Materials & Design, 32, (2011) 127.
[12] H. Zhu, Z. Zhang, K. Xu, J. Xu, S. Zhu, A. Wang, and H. Qi: Materials (Basel), 12, (2019) 41.
[13] S. Torres-Peiró, J. González-Ausejo, O. Mendoza-Yero, G. Mínguez-Vega, and J. Lan-cis: Appl. Surf. Sci., 303, (2014) 393.
[14] M.T. Li, M. Liu, and H.B. Sun: Phys. Chem. Chem. Phys., 21, (2019) 24262.
[15] B.N. Chichkov, C. Momma, S. Nolte, and F. von Alvensleben: Appl. Phys. A, 63, (1996) 109.
[16] B. Bhushan: Philos. Trans. A Math. Phys. Eng. Sci., 377, (2019) 20180274.
[17] M. Nosonovsky and B. Bhushan: "Green Tribology" (Springer, Berlin, 2008) pp.25-40.
[18] B. Bhushan: Langmuir, 28, (2012) 1698.
[19] H.F. Bohn and W. Federle: PANS, 101, (2004) 14138.
[20] C-P. Hsu, Y-M. Lin, and P-Y. Chen: JOM, 67, (2015) 744.
[21] P-G. de Gennes, F. Brochard-Wyart, and D. Quere: "Capillarity and wetting phenomena", (Springer Science+Business Media, Inc., New York, 2003) pp.13-15.
[22] D. Bradley, C.G.W. Sheppard, I.M. Suardjaja, and R. Woolley: Combust. Flame, 138, (2004) 55.
[23] S.S. Chhatre, W. Choi, A. Tuteja, K-C. Park, J.M. Mabry, G.H. McKinley, and R.E. Cohen: Scale dependence of omniphobic mesh surfaces, Langmuir, 26, (2010) 4027.
[24] M. Nosonovsky and B. Bhushan: Mater. Sci. Eng., 58, (2007) 162.
[25] M. Nosonovsky and B. Bhushan: Langmuir, 24, (2008) 1525.

(Received: April 21, 2020, Accepted: August 26, 2020)